

Spectral and polarization study of the double relics in Abell 3376 using the GMRT and the VLA

Ruta Kale^{1,2,3,4*}, K. S. Dwarkanath⁴, Joydeep Bagchi³, and Surajit Paul³

¹*Dipartimento di Astronomia, Università di Bologna, via Ranzani 1, I-40127 Bologna, Italy*

²*INAF-Istituto di Radioastronomia, Via Gobetti 101, I-40129 Bologna, Italy*

³*Inter University Centre for Astronomy and Astrophysics, Post Bag 4, Ganeshkhind, Pune University Campus, Pune 411007, India*

⁴*Raman Research Institute, C. V. Raman Avenue, Sadashivanagar, Bangalore 560080, India*

accepted in MNRAS

ABSTRACT

Double radio relics in galaxy clusters are rare phenomena that trace shocks in the outskirts of merging galaxy clusters. We have carried out a spectral and polarization study of the spectacular double relics in the galaxy cluster A3376 using the Giant Metrewave Radio Telescope at 150 and 325 MHz and the Very Large Array at 1400 MHz. The polarization study at 1400 MHz reveals a high degree of polarization ($\sim 30\%$) and aligned magnetic field vectors (not corrected for Faraday rotation) in the eastern relic. A highly polarized ($> 60\%$) filamentary radio source of size ~ 300 kpc near the eastern relic and north of the bent-jet radio galaxy is detected for the first time. The western relic is less polarized and does not show aligned magnetic field vectors. The distribution of spectral indices between 325 and 1400 MHz over the radio relics show steepening from the outer to the inner edges of the relics. The spectral indices of the eastern and the western relics imply Mach numbers in the range 2.2 to 3.3. Remarkable features such as the inward filament extending from the E-relic, the highly polarized filament, the complex polarization properties of the W-relic and the separation of the BCG from the ICM by a distance > 900 kpc are noticed in the cluster. A comparison with simulated cluster mergers is required to understand the complex properties of the double relics in the context of the merger in A3376. An upper limit ($\log(P_{1.4GHz} \text{ W Hz}^{-1}) < 23.0$) on the strength of a Mpc size radio halo in A3376 is estimated.

Key words: galaxies: clusters: individual: Abell 3376, acceleration of particles, radiation mechanisms: non-thermal, shock waves, radio continuum: general, X-rays: galaxies: clusters

1 INTRODUCTION

Clusters of galaxies, being the largest gravitationally bound structures in the Universe are interesting sites to study extreme phenomena. Evolution of galaxy clusters occurs through mergers of galaxy groups and galaxy sub-clusters involving dissipation of gravitational binding energies $\sim 10^{64}$ erg in the intra-cluster medium (ICM) via shocks and turbulence (Ryu et al. 2003). There is growing evidence that cluster-cluster mergers are connected to the presence of diffuse large scale radio sources called radio halos and radio relics (Ferrari et al. 2008). The channeling of the gravitational energy into the acceleration of particles and possibly amplification of the cluster magnetic field are not well understood and are currently the topics of active research.

Radio halos are \sim Mpc size radio sources, located co-spatially with the X-ray emission from the ICM. Acceleration of particles in the ICM through turbulence and production of relativistic electrons as secondary products of hadronic collisions in the ICM are the two mechanisms proposed for the generation of radio halos (see Brunetti 2011, and references therein).

Radio relics are elongated, polarized, filamentary and sometimes arc-like radio sources. One class of radio relics has been proposed to be remnants of radio galaxies evolving passively in the surrounding medium or revived by adiabatic compression by environmental shock waves (Enßlin & Gopal-Krishna 2001). The solitary filamentary relics of sizes $\sim 50 - 500$ kpc, sometimes located close to radio galaxies in clusters are likely to have these origins (Kale & Dwarkanath 2011). The radio relics of the other class have arc-like morphologies, \sim Mpc extents and are lo-

* E-mail: rkale@ira.inaf.it

cated at the peripheries of galaxy clusters. These are believed to be tracers of the cluster merger shocks or accretion shocks (Enßlin et al. 1998). The shocks are stronger toward the outskirts of clusters where the density of electrons is very low ($n_e < 10^{-4} \text{ cm}^{-3}$). Therefore, detecting them in X-rays is a challenge (Akamatsu & Kawahara 2011). The radio relics thus offer a unique window to trace the shocks and the ICM at cluster peripheries.

Shocks are known to accelerate electrons by the diffusive shock acceleration (DSA) mechanism and compress magnetic fields along the direction of propagation (Drury 1983). The DSA produces a power law distribution of relativistic electrons and thus provides a link between the spectral index of the radio emission and the strength of the shock. The alignment of magnetic fields results in polarized radio emission from radio relics. Thus, the integrated spectra, spectral index distribution and polarization of radio relics are crucial to find the properties of shocks in the ICM. However, radio relics are rare and only a handful of them are known. Therefore studying the properties of the known sources in as much detail as possible is important. Even rarer are the cases when the arc-like relics occur in pairs around galaxy clusters. Such relics occur in cluster-cluster mergers with the merger axes nearly in the plane of the sky. The effects of projection in studying the shocks and the merger in such a configuration are expected to be minimal. There are only nine clusters where such “double relics” have been discovered, namely, ZwCl 2341.1 + 0000 (Bagchi et al. 2002; van Weeren et al. 2009), A3376, PLCK G287.0 + 32.9 (Bagchi et al. 2002, 2006, 2011), A3667 (Rottgering et al. 1997), ZwCl 0008.8 + 5215, CIZA J2242.8 + 5301 (van Weeren et al. 2011c, 2010), RXCJ 1314.4 – 2515 (Feretti et al. 2005), A2345 (Giovannini et al. 1999; Bonafede et al. 2009) and A1240 (Kempner & Sarazin 2001; Bonafede et al. 2009). There are three more candidate double radio relics, namely 0217 + 70 (Brown et al. 2011), A3365 (van Weeren et al. 2011b) and A1758N (Giovannini et al. 2009).

In this paper we present a polarization and spectral study of the double relics in A3376 using the Giant Metrewave Radio Telescope (GMRT) and the Very Large Array (VLA). Abell 3376 is a nearby ($z = 0.046$) X-ray luminous ($L_X \sim 2 \times 10^{44} h_{70}^{-2} \text{ erg s}^{-1}$) cluster with spectacular double relics (Bagchi et al. 2006). It has an average temperature of $\sim 4 \text{ keV}$ and the X-ray surface brightness has a comet-like appearance which indicates the ongoing dynamical activity in the cluster. The virial mass of this cluster is estimated to be $\sim 3.64 \times 10^{14} h_{70}^{-1} M_\odot$ (Girardi et al. 1998). The two radio relics in A3376 are separated by a distance of $\sim 2 \text{ Mpc}$ and are located almost symmetrically around the X-ray emission from the ICM. The previous study of these relics at 1.4 GHz revealed the basic morphology of these relics and stated the possibilities that either outgoing cluster merger shocks or accretion shocks are responsible for the relics (Bagchi et al. 2006). In this paper we provide a more detailed description.

The paper is organised as follows. The observations and data reduction are described in section 2. The properties of the relics revealed from the radio images and the spectral index images are presented in section 3. In section 4 the implications of these properties are discussed. The work is summarized in section 5.

We adopt a Λ CDM cosmology with $H_0 = 71 \text{ km s}^{-1} \text{ Mpc}^{-1}$, $\Omega_M = 0.27$, and $\Omega_\Lambda = 0.73$, resulting in a scale

of $0.89 \text{ kpc arcsec}^{-1}$ for the redshift, 0.046 of A3376. The spectral index, α is defined as $S \propto \nu^\alpha$, where S is the flux density and ν , the frequency.

2 OBSERVATIONS AND DATA REDUCTION

The cluster A3376 was observed at 325 and 150 MHz with the GMRT in Nov. 2009 (proposal code 17_024, PI R. Kale). Two observing sessions of $\sim 7 \text{ hr}$ duration centered on the positions (J2000) RA 06h02m15s DEC -39d57m00s and RA 06h00m07s DEC -40d02m00s were conducted at 325 MHz. A bandwidth of 32 MHz was used. At 150 MHz, two observing sessions of $\sim 7 \text{ hr}$ duration with a bandwidth of 16 MHz were conducted. However data from one of the 150 MHz sessions were heavily corrupted by radio frequency interference (RFI) and had to be discarded.

The data at 150 and 325 MHz were analyzed using the standard procedures in NRAO Astronomical Image Processing System (AIPS) version 31DEC10. The VLA calibrator values (Perley-Butler 2010) were used for absolute flux calibration. Wide field imaging was carried out to account for the non-coplanarity of the array. The sensitivities at both 325 and 150 MHz were improved by several iterations of self-calibration. A single image was produced by combining images obtained from the data in the two observing sessions at 325 MHz. An image using the ‘natural’ weighting scheme (robust= 5 in AIPS) with a rms $2.0 \text{ mJy beam}^{-1}$ and a synthesized beam of $39'' \times 39''$ was produced at 325 MHz (Fig. 1). Similarly, an image with a rms $5.0 \text{ mJy beam}^{-1}$ and a synthesized beam of $47'' \times 47''$ was produced at 150 MHz (Fig. 2). High resolution images using the ‘uniform’ weighting scheme (robust= -5 in AIPS) were produced at both, 150 and 325 MHz to identify discrete radio sources.

Archival data from the VLA (proposal code AB1057, PI J. Bagchi) at 1400 MHz in the configurations CnB and DnC were analyzed. It consisted of separate pointings for each of the relics in the two configurations. Standard procedures of data editing, phase and flux calibration were carried out in AIPS (version 31DEC11). The calibrator source 0616 – 349 was used to obtain the polarization leakage terms and the source 3C286 was used to calibrate the polarization position angle. After calibration, the data in the two configurations for each of the relic were combined separately using the task ‘DBCON’. These visibilities were used to make stokes I, Q, U and V images. Self calibration was carried out to improve the sensitivities. The polarized intensity images were corrected for the Ricean bias using the task ‘POLCO’. Stokes I images (rms $\sim 40 \mu\text{Jy beam}^{-1}$) and Q and U images (rms $\sim 30 \mu\text{Jy beam}^{-1}$) were obtained (Fig. 3). The polarization vectors are not corrected for Faraday rotation.

The construction of spectral index distribution maps requires radio images at two frequencies with closely matched uv -plane sampling. Often, it is not possible to meet this requirement with a single radio telescope. The combination of the GMRT at 325 MHz and the VLA in CnB and DnC configurations at 1.4 GHz provides matched uv -coverages, sufficient to obtain spectral index distributions over the double relics in A3376. We obtained images with the uv -distances limited to 0.125–25 $k\lambda$ and the weighting scheme of robust= -5 (pure uniform) and uv -taper of $2k\lambda$ at both 325 and 1400 MHz. The uniform weights ensure same uv -

plane weighting distribution at the two frequencies. Primary beam gain corrections were applied and the regions with flux densities below 5σ were blanked. These images, convolved to a common resolution of $69'' \times 69''$ were used to construct the spectral index images and the corresponding uncertainty images (Fig. 4).

3 RESULTS: PROPERTIES OF THE DOUBLE RELICS

The cluster A3376 consists of two arc-like relics located almost symmetrically around the X-ray emission from the ICM (Fig. 1). We will henceforth refer to the relic to the east of the X-ray emission as E-relic and the one to the west as the W-relic.

The E-relic can be divided into three regions- an arc-like southern region, a relatively faint northern region and a filament extending into the cluster (Fig. 1). The southern arc has a sharp outer edge and a width in the range $\sim 50 - 200$ kpc. A fractional polarized intensity of up to 30% is detected in it and the magnetic field vectors (uncorrected for Faraday rotation) are aligned parallel to the elongation of the arc (Fig. 3, left). A steep gradient of spectral indices (-0.7 to -1.3) from the outer to the inner edge is seen (Fig. 4, top left). The northern portion of the E-relic has steeper spectral indices (-1 to -1.5) and does not show a sharp edge. There is a striking inward extending filament from the E-relic, creating a ‘notch’ in the overall arc-like shape of the E-relic. It has a linear extent of ~ 500 kpc and a steep spectral index (~ -1.5). In the higher resolution ($20'' \times 20''$) image at 1.4 GHz, the southern arc is prominent and the northern region together with part of the inward filament forms another arc (see Fig. 1B in Bagchi et al. 2006). The inward filament and this arc connect to each other forming a loop. These details are not resolved in the 325 MHz image presented here. It is clear that the E-relic, though apparently arc-like, has many other complex structures associated with it, which require further study to understand their real nature. The differences in spectral indices of the various regions can also lead to differences in the morphology at widely separated frequencies such as 150 - 1400 MHz. The regions of the E-relic having steeper spectra are detected in the 150 MHz image with higher significance than the southern arc prominent in 325 and 1400 MHz images (Fig. 2).

The polarized intensity map of the E-relic also reveals a filament showing high fractional polarization ($> 60\%$) located north of the bent-jet radio galaxy (Fig. 3, left). The magnetic field vectors in this filament are also aligned approximately parallel to those in the southern arc of the E-relic.

The outer edge of the W-relic also follows the curvature of the E-relic like a mirror image. The W-relic has a largest extent of ~ 900 kpc and has a maximum width of ~ 300 kpc near the center (Fig. 1). It is also polarized between 5 to 20% in a few pockets but does not show alignment of magnetic field vectors in any single direction (Fig. 3, right). This may be an effect of Faraday rotation by the magnetized ICM. The distribution of spectral indices shows flatter spectra toward the outer edge as compared to the inner edge (Fig. 4, bottom left). Arc-like radio relics typically show monotonically decreasing surface brightness from their outer to inner

Table 1. Flux densities and spectral indices of the A3376 relics.

	E-relic	W-relic
S_{1400} (mJy)	122 ± 10	113 ± 10
S_{325} (mJy)	1770 ± 90	1367 ± 70
S_{150} (mJy)	3500 ± 350	2962 ± 300
α_{325}^{325}	-0.88 ± 0.14	-1.00 ± 0.14
α_{325}^{1400}	-1.82 ± 0.06	-1.70 ± 0.06

edges. However, the surface brightness of the W-relic shows a depression by a factor of ~ 2 at its center. A larger error (~ 0.3) corresponding to this lower surface brightness region is seen in the spectral index uncertainty image (Fig. 4, bottom right). The W-relic at 150 MHz lacks the arc-like outer edge that is seen at both 325 and 1400 MHz (Fig. 2).

The integrated flux densities and spectral indices of the relics are summarized in Table 1. The flux densities at 325 MHz and 150 MHz were obtained from the images in Fig. 1 and Fig. 2 respectively. The images at 1400 MHz, using $\text{robust}=5$ (not shown), were used. The contribution of unresolved sources estimated from high resolution images were subtracted to obtain the estimates of the flux densities of the relics. Both the relics show high frequency steepening in their spectra. The largest detectable extent with the VLA at 1400 MHz ($\sim 18'$) is close to the largest extents of the relics in the \sim north-south direction. There may be some loss of flux density at 1400 MHz due to this resulting in an apparently steep spectral index between 325- 1400 MHz.

4 DISCUSSION

The cluster A3376 is a spectacular massive, merging cluster of galaxies. The galaxy distribution shows at least two sub-clusters located along the axis of elongation of the X-ray surface brightness (Flin & Krywult 2006). The giant ring-like radio relics at the outskirts of the cluster are located along the same axis. The alignment of magnetic field vectors in the E-relic and the spectral index steepening toward inner edges of the relics support the scenario of shock acceleration at the radio relics.

The acceleration of electrons at the shock by DSA results in a power law spectrum of the electrons. In a fully ionized plasma the slope of the power law spectrum, δ_{inj} , is related to the Mach number, M , of the shock as given by (e.g. Blandford & Eichler 1987),

$$\delta_{inj} = -2 \frac{M^2 + 1}{M^2 - 1} \quad (1)$$

The spectral index of the accelerated electrons is $\alpha_{inj} = (\delta_{inj} + 1)/2$. If we assume that the shock is located at the radio relics and that the synchrotron and inverse Compton losses have not affected the spectrum of the accelerated electrons, then the flattest spectrum will represent the spectral index at injection. The flattest spectral index in the southern arc in the E-relic as read from the spectral index map is -0.70 ± 0.15 (Fig. 4, top left). The implied Mach number is 3.31 ± 0.29 . The spectral index at the outer edge of the W-relic is -1.0 ± 0.2 and the implied Mach number is 2.23 ± 0.40 (Fig. 4, bottom left). These Mach numbers imply

that the shocks at the relics are cluster merger shocks and not accretion shocks ($M > 10$).

Deep X-ray observations with sensitive instruments can provide an independent measure of the properties of shocks through the measurements of temperature and pressure jumps at the location of radio relics. The *SUZAKU* X-ray observations of A3376 by Akamatsu et al. (2011) reveal temperature and pressure jumps across the W-relic. A temperature jump from 1.35 ± 0.35 keV in the pre-shock region to 4.81 ± 0.29 keV in the post-shock region is reported at the W-relic. They find Mach numbers of 2.94 ± 0.60 and 4.78 ± 0.49 from the temperature and pressure jumps, respectively. The radio Mach number of the W-relic is consistent with the one calculated using the temperature jump. The Mach number estimated from the pressure jump is less reliable due to the assumptions, such as of spherical symmetry, that are used in the determination of the electron density profile (Akamatsu et al. 2011).

In the process of structure formation, large scale shocks are driven into the diffuse medium. High Mach number shocks ($M > 10$) are formed in filaments surrounding the virializing cores of clusters. On the other hand, low Mach number ($M < 10$) shocks are formed in the clusters. Most of the kinetic energy of the accreted matter is dissipated by the relatively low Mach number shocks ($M < 4$) (Miniati et al. 2000; Ryu et al. 2003). These Mach numbers are consistent with those found from the spectral indices of the A3376 radio relics and also other relics (van Weeren et al. 2010; Finoguenov et al. 2010). These findings imply shock velocities ~ 1000 km s⁻¹ at the radio relics. This shock velocity is comparable to that in supernova remnants, however the Mach numbers are much lower (Jones 2012). The low Mach number shocks are believed to be inefficient in accelerating electrons from the thermal ICM to relativistic energies as required to produce the radio relics (Kang & Jones 2002). Thus the understanding of the generation of relativistic electrons through DSA at such low Mach number shocks is still incomplete. Nevertheless the coincidence of such shocks with the radio relics does imply their role in the reacceleration of a pre-existing population of relativistic electrons or in strengthening the magnetic fields.

4.1 Remarkable features of A3376

The spectral and polarization study of double radio relics in A3376 has revealed several new features. The properties of the A3376 relics such as – aligned polarization vectors and spectral steepening from outer to inner edges, are similar to the radio relics in other galaxy clusters. Majority of the single and double relics at cluster outskirts have been found to be located along the direction of elongation of the X-ray surface brightness (van Weeren et al. 2011b). The A3376 relics are in line with this property of other relics as well.

However there are some remarkable properties of the relics in A3376 and of the cluster itself that we have noticed. The ~ 500 kpc long inward filament of the E-relic is a peculiar feature. It has a width of ~ 300 kpc and has steep spectral index. Backflows from shock fronts, under standard assumptions can have maximum widths of up to ~ 200 – 250 kpc (Brunetti et al. 2008). The widths of radio relics have been explained as due to such back flows (Brunetti et al. 2008; van Weeren et al. 2010). However the inward filament

in A3376 is different from such a backflow in that it extends from only a section of the E-relic, creating a ‘notch’ at that location. A possibility that the ‘notch’ may be due to the breakup of the shock front in an encounter with a filament has been expressed recently (Paul et al. 2011).

A highly polarized filament of extent $\sim 300 \times 50$ kpc² north of the bent-jet radio galaxy with magnetic fields aligned in the same direction as in the southern arc of the E-relic is revealed for the first time. This polarized filament is located ~ 200 kpc behind the northern part of the E-relic as projected in the sky plane.

The W-relic, though has an arc-like morphology at the edge, lacks an aligned magnetic field. It is possible that the turbulence in the backflow of the shock has resulted in the complex geometry of the field. Faraday rotation by the ICM can rotate the polarization vectors. The relics are located outside the dense part of the ICM (Fig. 1) and thus this effect is expected to be small (Clarke 2004). Deeper observations mapping the polarized emission and a model for the ICM density in A3376 are required.

There are two prominent galaxies in A3376. One is the brightest cluster galaxy (BCG), ESO 307-13, and the other is the bent-jet radio galaxy near the peak of the X-ray emission, MRC 0600 – 399 (Fig. 1). Most cD galaxies and BCGs are located at the cores of galaxy clusters with dense ICM surrounding them (Bautz & Morgan 1970). Many of those are powerful radio galaxies and play a major role in heating of the ICM. The BCG in A3376 is unique due to its separation of > 900 kpc from the peak of X-ray surface brightness. The powerful cluster-cluster merger in A3376 may have led to a setting in which the BCG is ‘orphaned’. Simulation studies may be able to point out the details of a merger which can result in BCG-ICM peak separation as large as > 900 kpc. Mapping of dark-matter distribution in A3376 with the gravitational lensing method is likely to shed additional light on the complex merger dynamics.

A3376 is well suited for a detailed comparison with simulated cluster mergers, given that it is a well studied cluster at X-rays, optical and radio wavelengths (Akamatsu et al. 2011; Flin & Krywult 2006; Bagchi et al. 2006, and present work). Details of the merger geometry and the properties of individual sub-clusters can be obtained by matching simulations with observations as has been carried out in the case of the cluster CIZA J2242.8+5301 (van Weeren et al. 2011a). The double relics in CIZA J2242.8+5301 fit the picture of outgoing merger shocks and have been modelled by a toy model of cluster merger shocks. However, in the case of A3376, due to the morphological details of the E and W-relics which indicate an interaction with the large scale structure filaments, a cluster merger in a cosmological simulation will be more appropriate. This will provide further insights into the formation of the double relics in A3376 and cluster mergers in general.

4.2 A Radio halo in A3376?

Radio halos are diffuse radio sources that trace relativistic electrons and magnetic fields in galaxy cluster centers. Like the relics, they are also rare and have been found to occur preferentially in clusters undergoing mergers (Cassano et al. 2010). It is still not understood why certain merging clusters have radio relics whereas others have radio halos. Also

there are cases where single radio relics and radio halos are in the same cluster. It is important to understand whether the formation of a radio halo and of radio relics in a galaxy cluster is simultaneous or it is separated in time. This will provide an insight into the details of the underlying mechanisms of their generation in cluster mergers. In this context, we examined whether A3376 has a radio halo. No emission from a radio halo is detected in the 150, 325 and 1400 MHz images. To obtain upperlimits on the radio power of radio halos a method of injection of fake radio halos has been used (for e.g. Venturi et al. 2008; Brunetti et al. 2007). We used AIPS task ‘UVSUB’ to inject uniform spherical halos of total flux densities in the range 50 to 500 mJy in the 325 MHz data. The radius of the injected halo was 500 kpc and the location RA 06h01m20.52s DEC -39d59m50.8 (J2000), which is approximately midway between the two relics. We found that a radio halo of 100 mJy at the level of suspecting diffuse emission (positive residuals) was detected. Using this as a limiting flux density of detection at 325 MHz, if we assume a spectral index of -1.0 over the frequency range 325 - 1400 MHz, a limit on the radio power of 1.02×10^{23} W Hz⁻¹ is obtained at 1400 MHz. A radio power of 1.91×10^{23} W Hz⁻¹ at 1.4 GHz is expected if A3376 were to follow the X-ray luminosity and 1.4 GHz power correlation for giant radio halos (Cassano et al. 2006). The upperlimit is a factor of ~ 2 below the expected radio halo power. Therefore in the picture of radio halo evolution, this may be either an early stage of halo formation or a fading stage after attaining the peak radio power.

5 SUMMARY

We have presented a polarization and spectral index study of the double radio relics in the cluster A3376. The findings from this study can be summarized as follows:

(i) Images of the double relics in A3376 were obtained at 150 and 325 MHz with the GMRT and at 1400 MHz with the VLA. The integrated spectra of both the relics show steepening in the frequency range 325 - 1400 MHz as compared to 150 - 325 MHz.

(ii) The spectral index distribution (325-1400 MHz) shows flatter spectra at the outer edges of both the relics as compared to their inner edges. The Mach numbers implied by the spectral indices of the relics range between 2.2 - 3.3.

(iii) The eastern relic is polarized up to 30% and shows aligned magnetic field vectors as expected in a shock. The western relic is relatively less polarized and shows complex orientations of the magnetic fields.

(iv) The polarization map also reveals a highly polarized filament located behind the eastern relic as projected in the sky plane, for the first time.

(v) A steep spectrum filament of size 500 kpc extends inward from the eastern relic creating a ‘notch’ at the outer edge of the relic. Such a structure cannot be explained easily in the standard outgoing shock model for the double relics.

(vi) An upperlimit on the power of a Mpc size radio halo ($\log(P_{1.4GHz}) < 23.0$) is obtained.

(vii) It is also noted that the brightest galaxy in A3376 is located ~ 900 kpc away from the peak of the X-ray emission

from the cluster –possibly ‘orphaned’ by the ongoing merger in the cluster.

The radio, X-ray and optical properties of the cluster point toward a major merger in A3376. The polarization and spectral properties of the relics support the outgoing merger shock model. A comparison of the properties of A3376 with that of simulated cluster mergers will lead to a better understanding of the details of the sub-clusters involved in the merger.

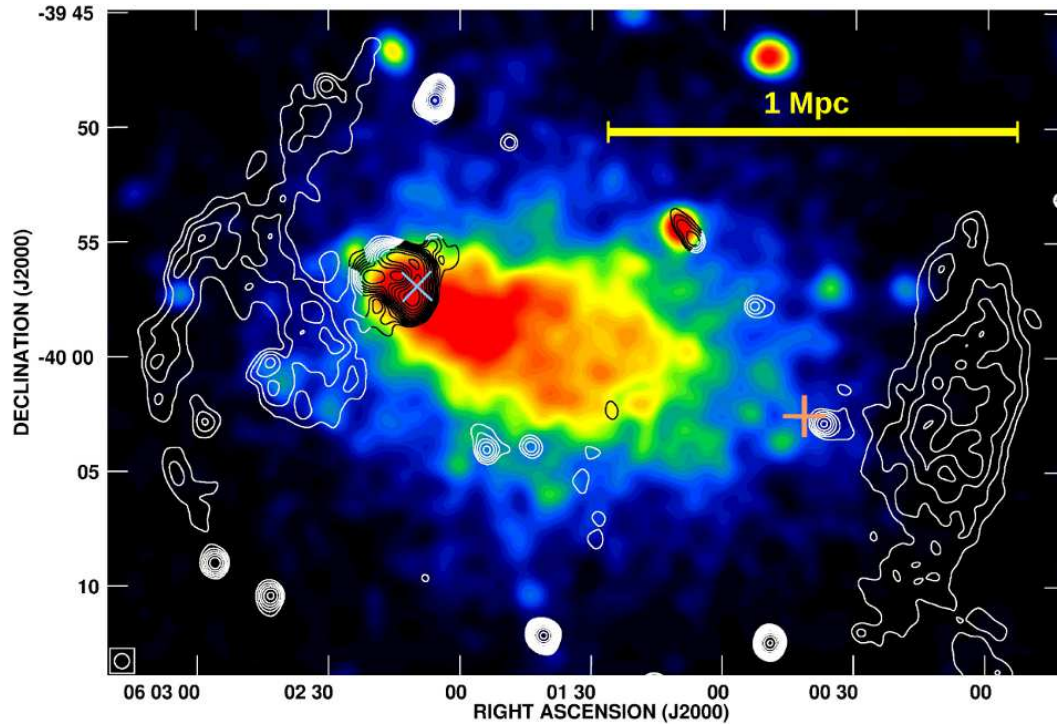


Figure 1. The GMRT 325 MHz image is shown in contours. The contour levels start $5.8 \text{ mJy beam}^{-1}$ and increase by a factor of $\sqrt{2}$. The synthesized beam is $39'' \times 39''$. The ROSAT soft X-ray band image (0.1-2.4 keV) is shown in color. The 'x' and the '+' signs mark the positions of the galaxies MRC 0600 – 399 (bent double radio galaxy) and ESO 307 – 13 (BCG), respectively.

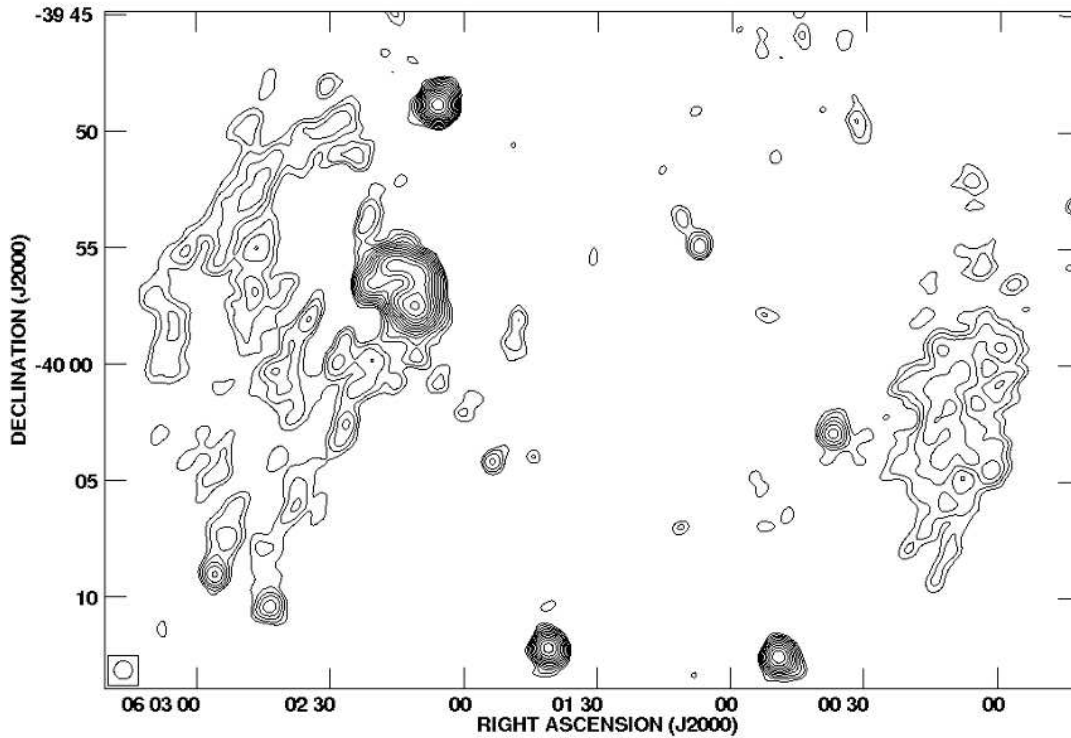


Figure 2. The GMRT 150 MHz image is shown in contours. The contour levels start at $15.0 \text{ mJy beam}^{-1}$ and increase by a factor of $\sqrt{2}$. The synthesized beam is $47'' \times 47''$.

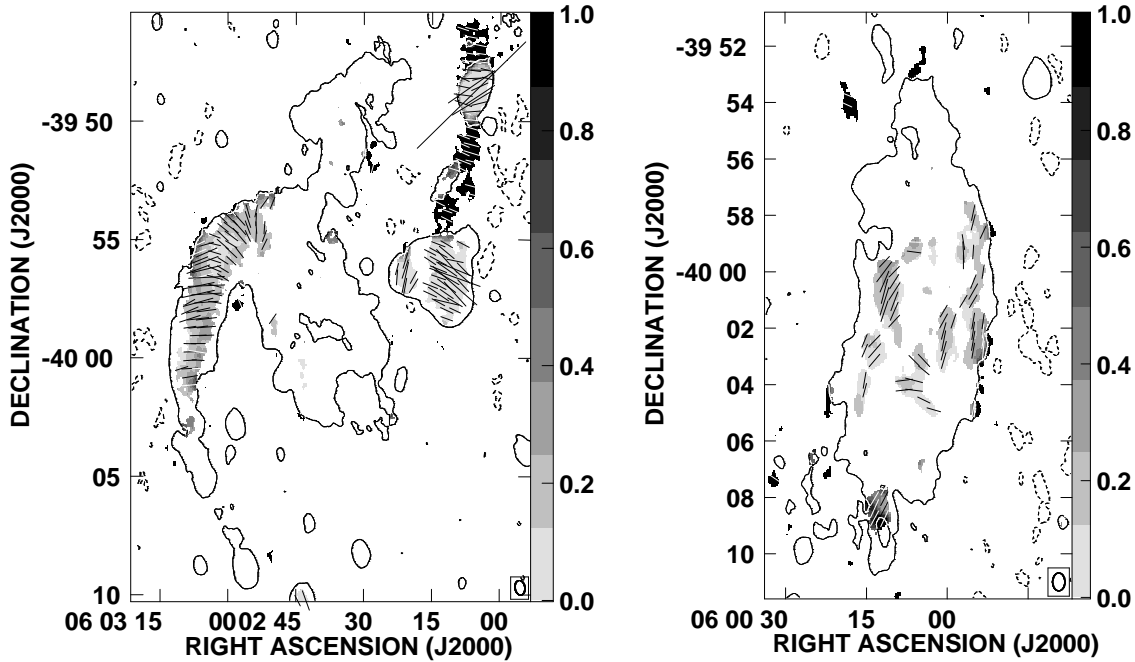


Figure 3. VLA 1400 MHz: Electric field vectors overlaid on fractional polarized intensity shown in grey-scale and Stokes I contours shown at $-0.16, 0.16 \text{ mJy beam}^{-1}$. The length of the vectors is proportional to the polarized intensity. The synthesized beam is $37'' \times 25''$ (P. A. 9.22°) in the left panel and $38'' \times 26''$ (P. A. 0.17°) in the right panel.

ACKNOWLEDGMENTS

We thank the anonymous referee for providing comments that have improved this paper. We thank the staff of the GMRT who have made these observations possible. GMRT is run by the National Centre for Radio Astrophysics of the Tata Institute of Fundamental Research. The National Radio Astronomy Observatory is a facility of the National Science Foundation operated under cooperative agreement by Associated Universities, Inc. This research has made use of the NASA/IPAC Extragalactic Database (NED) which is operated by the Jet Propulsion Laboratory, California Institute of Technology, under contract with the National Aeronautics and Space Administration. We have made use of the ROSAT Data Archive of the Max-Planck-Institut für extraterrestrische Physik (MPE) at Garching, Germany.

REFERENCES

- Akamatsu H., Kawahara H., 2011, ArXiv e-prints
 Akamatsu H., Takizawa M., Nakazawa K., Fukazawa Y., Ishisaki Y., Ohashi T., 2011, ArXiv e-prints
 Bagchi J., Durret F., Neto G. B. L., Paul S., 2006, *Science*, 314, 791
 Bagchi J., Enßlin T. A., Miniati F., Stalin C. S., Singh M., Raychaudhury S., Humeshkar N. B., 2002, ArXiv e-prints, 7, 249
 Bagchi J., Sirothia S. K., Werner N., Pandge M. B., Kantharia N. G., Ishwara-Chandra C. H., Gopal-Krishna, Paul S., Joshi S., 2011, *ApJ*, 736, L8
 Bautz L. P., Morgan W. W., 1970, *ApJ*, 162, L149
 Blandford R., Eichler D., 1987, *Phys. Rep.*, 154, 1
 Bonafede A., Giovannini G., Feretti L., Govoni F., Murgia M., 2009, *A&A*, 494, 429
 Brown S., Duisterhoeft J., Rudnick L., 2011, *ApJ*, 727, L25
 Brunetti G., 2011, *MMSAI*, 82, 515
 Brunetti G., Giacintucci S., Cassano R., Lane W., Dallacasa D., Venturi T., Kassim N. E., Setti G., Cotton W. D., Markevitch M., 2008, *Nature*, 455, 944
 Brunetti G., Venturi T., Dallacasa D., Cassano R., Dolag K., Giacintucci S., Setti G., 2007, *ApJ*, 670, L5
 Cassano R., Brunetti G., Setti G., 2006, *MNRAS*, 369, 1577
 Cassano R., Etori S., Giacintucci S., Brunetti G., Markevitch M., Venturi T., Gitti M., 2010, *ApJ*, 721, L82
 Clarke T. E., 2004, *Journal of Korean Astronomical Society*, 37, 337
 Drury L. O., 1983, *Rep. on Progress in Phys.*, 46, 973
 Enßlin T. A., Biermann P. L., Klein U., Kohle S., 1998, *A&A*, 332, 395
 Enßlin T. A., Gopal-Krishna, 2001, *A&A*, 366, 26
 Feretti L., Schuecker P., Böhringer H., Govoni F., Giovannini G., 2005, *A&A*, 444, 157
 Ferrari C., Govoni F., Schindler S., Bykov A. M., Rephaeli Y., 2008, *Space Sci. Rev.*, 134, 93
 Finoguenov A., Sarazin C. L., Nakazawa K., Wik D. R., Clarke T. E., 2010, *ApJ*, 715, 1143
 Flin P., Krywult J., 2006, *A&A*, 450, 9
 Giovannini G., Bonafede A., Feretti L., Govoni F., Murgia M., Ferrari F., Monti G., 2009, *A&A*, 507, 1257
 Giovannini G., Tordi M., Feretti L., 1999, *New Astr. Rev.*, 4, 141
 Girardi M., Giuricin G., Mardirossian F., Mezzetti M., Boschini W., 1998, *ApJ*, 505, 74
 Jones T. W., 2012, *JApA*, 33
 Kale R., Dwarakanath K. S., 2011, *ApJ*, 744, 46

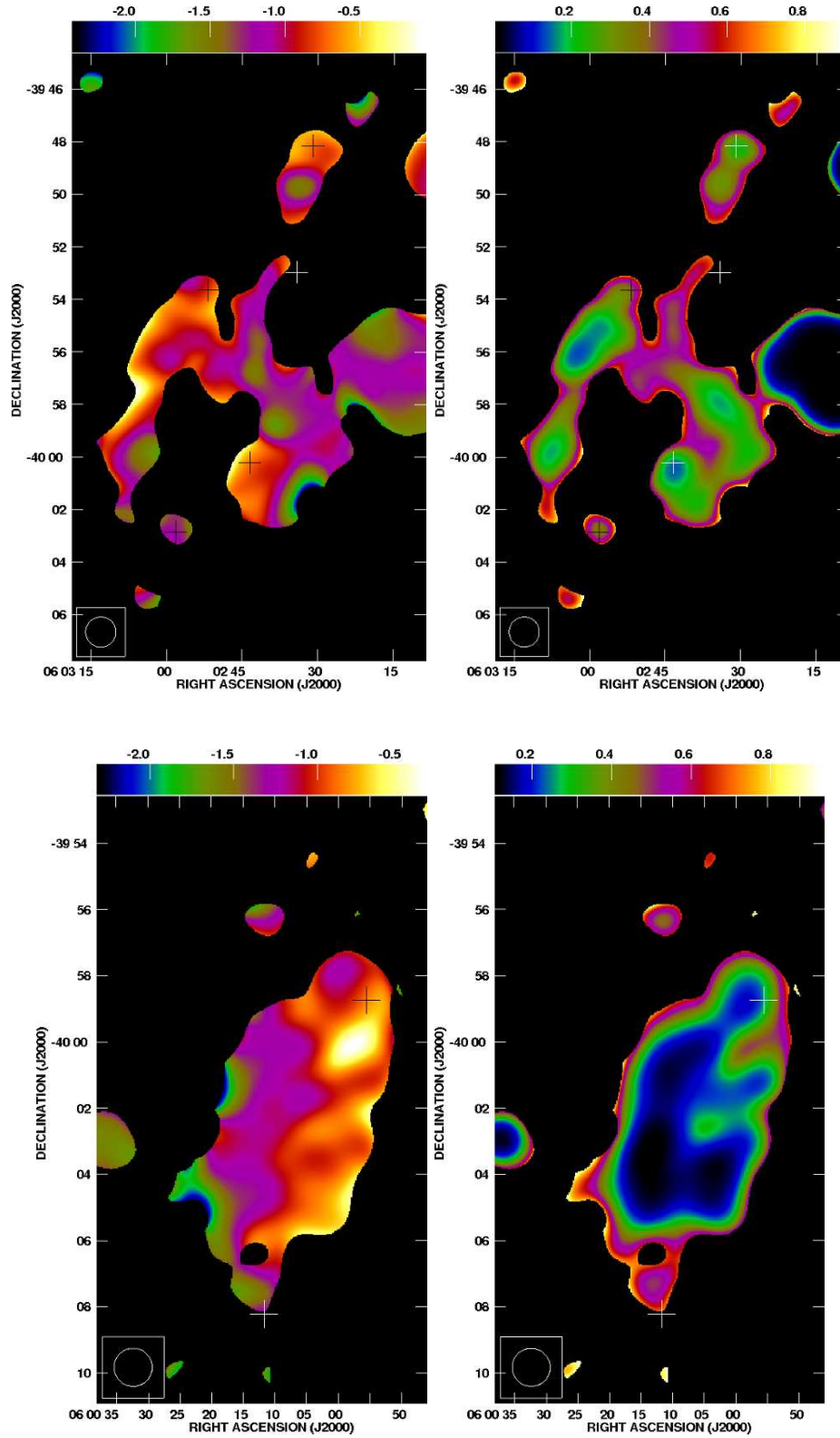


Figure 4. The top two panels show the spectral index map between 325 and 1400 MHz (left) and the corresponding uncertainty map (right) for the E-relic in colour. The bottom two panels show the same for the W-relic. The synthesized beam is $69'' \times 69''$ in all the panels. The crosses mark the positions of peaks of the compact sources in the regions of the relics, detected in the 1400 MHz images.

- Kang H., Jones T. W., 2002, JKAS, 35, 159
Kempner J. C., Sarazin C. L., 2001, ApJ, 548, 639
Miniati F., Ryu D., Kang H., Jones T. W., Cen R., Ostriker J. P., 2000, ApJ, 542, 608
Paul S., Iapichino L., Miniati F., Bagchi J., Mannheim K., 2011, ApJ, 726, 17
Röttgering H. J. A., Wieringa M. H., Hunstead R. W., Ekers R. D., 1997, MNRAS, 290, 577
Ryu D., Kang H., Hallman E., Jones T. W., 2003, ApJ, 593, 599
van Weeren R. J., Brüggen M., Röttgering H. J. A., Hoeft M., 2011a, MNRAS, 418, 230
van Weeren R. J., Brüggen M., Röttgering H. J. A., Hoeft M., Nuza S. E., Intema H. T., 2011b, A&A, 533, A35
van Weeren R. J., Hoeft M., Röttgering H. J. A., Brüggen M., Intema H. T., van Velzen S., 2011c, A&A, 528, A38
van Weeren R. J., Röttgering H. J. A., Bagchi J., Raychaudhury S., Intema H. T., Miniati F., Enßlin T. A., Markevitch M., Erben T., 2009, A&A, 506, 1083
van Weeren R. J., Röttgering H. J. A., Brüggen M., Hoeft M., 2010, Science, 330, 347
Venturi T., Giacintucci S., Dallacasa D., Cassano R., Brunetti G., Bardelli S., Setti G., 2008, A&A, 484, 327

This paper has been typeset from a $\text{\TeX}/\text{\LaTeX}$ file prepared by the author.